

## Physics-Informed Machine Learning for Solder Joint Qualification Tests

de Jong, S.D.M.; Ghezeljehmeidan, A.G.; van Driel, W.D.

**DOI**

[10.1109/EuroSimE60745.2024.10491412](https://doi.org/10.1109/EuroSimE60745.2024.10491412)

**Publication date**

2024

**Document Version**

Final published version

**Published in**

Proceedings of the 2024 25th International Conference on Thermal, Mechanical and Multi-Physics Simulation and Experiments in Microelectronics and Microsystems (EuroSimE)

**Citation (APA)**

de Jong, S. D. M., Ghezeljehmeidan, A. G., & van Driel, W. D. (2024). Physics-Informed Machine Learning for Solder Joint Qualification Tests. In *Proceedings of the 2024 25th International Conference on Thermal, Mechanical and Multi-Physics Simulation and Experiments in Microelectronics and Microsystems (EuroSimE)* (2024 25th International Conference on Thermal, Mechanical and Multi-Physics Simulation and Experiments in Microelectronics and Microsystems, EuroSimE 2024). IEEE. <https://doi.org/10.1109/EuroSimE60745.2024.10491412>

**Important note**

To cite this publication, please use the final published version (if applicable). Please check the document version above.

**Copyright**

Other than for strictly personal use, it is not permitted to download, forward or distribute the text or part of it, without the consent of the author(s) and/or copyright holder(s), unless the work is under an open content license such as Creative Commons.

**Takedown policy**

Please contact us and provide details if you believe this document breaches copyrights. We will remove access to the work immediately and investigate your claim.

***Green Open Access added to TU Delft Institutional Repository***

***'You share, we take care!' - Taverne project***

**<https://www.openaccess.nl/en/you-share-we-take-care>**

Otherwise as indicated in the copyright section: the publisher is the copyright holder of this work and the author uses the Dutch legislation to make this work public.

# Physics-Informed Machine Learning for Solder Joint Qualification Tests

S.D.M. de Jong<sup>1</sup>, A.G. Ghezeljehmeidan<sup>1</sup>, W.D. van Driel

Department of Microelectronics, Delft University of Technology, Delft, Netherlands  
Mekelweg 4, 2628 CD Delft, Netherlands.

S.D.M.deJong@tudelft.nl and amir.ghorbani@tudelft.nl and willem.vandriel@tudelft.nl

## Abstract

The ability to accurately predict the reliability and lifetime of electronics is of great importance to the industry. The failure of the solder joint is of particular interest for these predictions, because of their susceptibility to failure under thermo-mechanical stress. However, the experimental or even conventional simulation techniques employed to estimate the lifetime of a solder joint are often too expensive or time consuming to be of practical use. Therefore, this work introduces a physics-informed Long Short-Term Memory (LSTM) to predict the plastic strain in the critical area of the solder joint. The predicted values are in agreement with the values gained from finite elements, thereby demonstrating the advantage of applying the proposed methodology.

Keywords: Solder Joint Reliability, Plasticity, Finite Elements, PINN, LSTM

## 1. Introduction

Electronics are ever-present in industry and personal use. Therefore, the reliability of the electronic packaging is of utmost importance. A popular means of packing is currently Wafer Level Packaging (WLP) due to its low cost, small size and suitability for batch manufacturing. Reliability issues in WLP arises mainly due to the difference in Coefficient of Thermal Expansion (CTE) of the chip and the substrate. As the temperature increases and the materials expand, the differences in CTE results in stresses and strains. In the solder joint this can lead to significant plastic deformation. When the thermal load is cyclical the incremental plastic strain can lead to fatigue failure in the solder joint.

A common method to evaluate the reliability of the WLP is to conduct Accelerated Thermal Cycling Tests (ATCT). These ATCT are expensive and time consuming to perform, the Finite Element Method (FEM) has therefore seen widespread use for faster reliability predictions at a reduced cost [1, 2, 3]. However, these FEM simulation are not without problems of their own. The simulation require a lot of computing power, a large amount of memory, and the computational cost increases with model complexity. The scale of this becomes unmanageable for complex problems, or for which a large number of simulations are necessary. In recent years, Artificial Intelligence

(AI) has become a promising area of research to address these issues. Various Machine Learning (ML) techniques have been applied to the reliability of microelectronics, for example Supported Vector Regression (SVR) [4, 5], Random Forest (RF) [4, 6], and a range of different neural networks [4, 7, 8]. The majority of these papers extend the lifetime of equipment by focusing on optimizing the geometry under specified thermal conditions. The methods developed can be used during the design of the WLP, but have little use after the design phase.

Within this study a Deep Neural Network (DNN) is used. Deep neural networks are general models that can be trained to solve scientific computing problems. In a typical DNN each module computes nonlinear input-output mappings and this transformation makes it suitable as a universal functions approximator [9]. Long Short-Term Memory (LSTM) networks have become a cornerstone of deep learning for sequential data processing. Unlike traditional Recurrent Neural Networks (RNNs) that struggle with capturing long-range dependencies, LSTMs boast a sophisticated architecture specifically designed to overcome this limitation. At the core of an LSTM lies a fundamental unit called a memory cell. This cell departs from the simplistic activation functions of standard RNNs and incorporates a complex gating mechanism. These gates, namely the forget gate, input gate, and output gate, act as intelligent data flow regulators within the cell. This intricate gating mechanism empowers LSTMs to learn and remember long-term dependencies within sequences. The information persists across multiple time steps, enabling the network to effectively analyze data with temporal relationships.

Additionally, the new learning philosophy called physics-informed neural networks (PINNs) [10] has been introduced for the solution of nonlinear partial differential equations which governs the physics of system [11]. While training in DNN generally required a large amount of data, physics embedding by incorporating governing equations and initial or boundary conditions in the training stage can enhance the robustness and dependability of learning from physical data obtained via analytical or high-fidelity numerical solutions.

In this work, the LSTM network is employed on a WLP with a fixed geometry under variable thermal conditions. By doing this the equivalent plastic strain  $\varepsilon_{eq}^p$  in the solder joint can be found as a function of time  $t$ .

<sup>1</sup>These two authors contribute equally to the work.

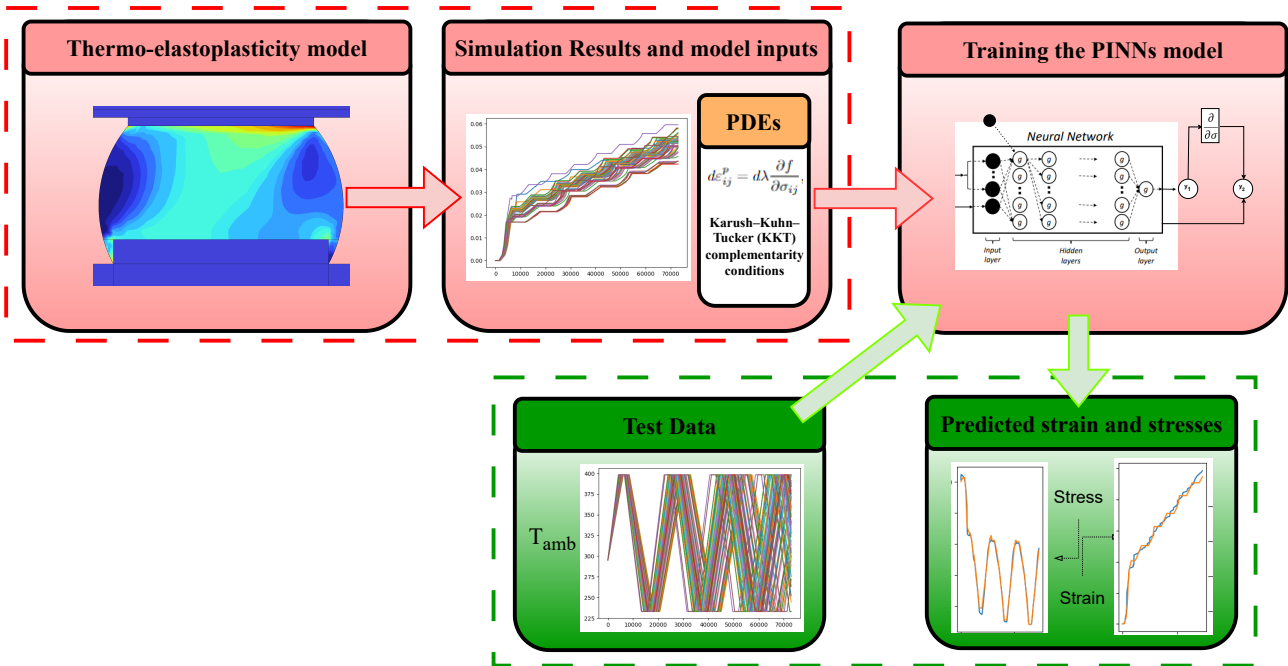


Fig. 1: overview of the model combined with the FEM analysis.

## 2. Methodology

### A. Dimensions and Materials

A two-dimensional slice of the WLP is used in this work to reduce the computational cost of the simulation. This is possible because the failure happens furthest away from the center of the WLP[5]. All simulations in this work are performed on single geometric design, the width and height of which has been given in Table 1 for each of the different components.

TABLE 1: The dimensions of the WLP.

Component	Dimensions [ $\mu\text{m}$ ]
Si Chip	2000 x 330
Cu Pad	220 x 25
SBL 1	2000 x 8
SBL 2	2000 x 7.5
UBM	190 x 8.6
PCB	3900 x 1000
Ball Diameter	250

As mentioned before, the cause of failures in the WLP are primarily caused by the difference in material properties of different components. The properties of the materials used in the WLP are shown in Table 2. A few assumptions were made about the materials to simplify the simulations. The materials are assumed to be homogeneous and isotropic, and the material properties are independent of temperature, with the notable exception of the Young's Modulus of solder ball material. The material used for the solder ball is SAC305, the properties of which are shown in Figure 2.

TABLE 2: The Material properties for the WLP.

Material	Youngs Modulus [GPa]	Poisson Ratio	CTE [ppm/ $^{\circ}\text{C}$ ]
Si Chip	129	0.28	2.62
Cu	68.9	0.34	16.7
SBL	2	0.33	55
PCB	18.2	0.30	23.9
Solder Ball	Non-Linear	0.35	25

### B. Thermal Cycling Conditions

The thermal cycling conditions employed in this work are based upon the well known JEDEC standards. The temperature cycle consists of a ramp rate, i.e. the rate at which the temperature increases and decreases, a maximum

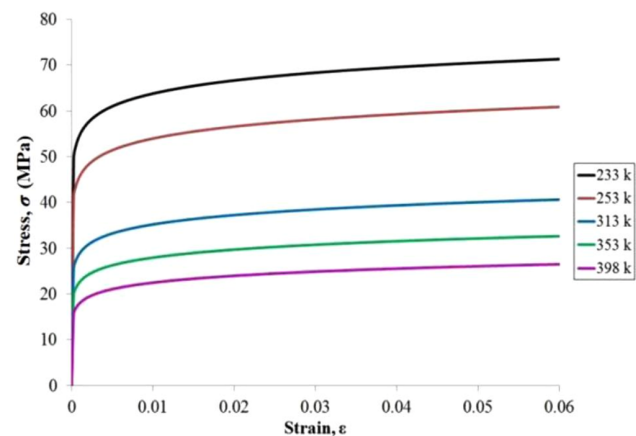


Fig. 2: Non-linear material properties of SAC305 for different temperatures[6].

temperature, a minimum temperature and a dwell time to ensure a uniform temperature distribution. An example of a temperature cycle is shown in Figure 3 is for the JEDEC standard JESD22-A104D Condition G, with temperature ranges from  $-40^{\circ}\text{C}$  to  $125^{\circ}\text{C}$ .

The plastic strain that occurs due to the thermal strain in the solder joint is dependent on the parameters of the cycles. Of those the ramp rate has the most effect on the failure in the solder joint. Therefore, different ramp rates, ranging between  $10^{\circ}\text{C}/\text{min}$  and  $15^{\circ}\text{C}/\text{min}$  are simulated in order to be used as training, validation and testing data for the machine learning section of this work.

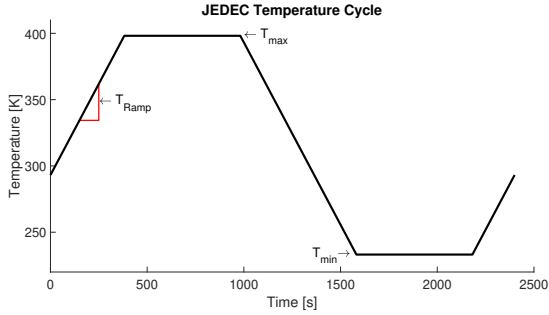


Fig. 3: Example of a JEDEC temperature cycle

### C. Fundamentals of Plasticity

The solder ball material SAC305 is modeled using elastoplastic behaviour. A material behaves elastic as long as the yield stress  $\sigma_y$  is not exceeded, and plastic when the stress is larger. Mathematically this can be expressed as

$$f(\sigma_{ij}, h, T) + df \leq 0 \quad \text{Elastic}, \quad (1)$$

$$f(\sigma_{ij}, h, T) + df > 0 \quad \text{Plastic}, \quad (2)$$

where  $f$  is the yield function,  $\sigma_{ij}$  the relevant stress,  $h$  determines the hardening in the material, and  $T$  the temperature. When the stress is equal to the yield stress, i.e.  $f = 0$ , and the increment is larger than zero, plasticity occurs. The increments of plastic strain can be calculated from the flow rule given as

$$d\varepsilon_{ij}^p = d\lambda \frac{\partial f}{\partial \sigma_{ij}}, \quad (3)$$

where  $\lambda$  is the plastic multiplier subject to  $\lambda \geq 0$  and  $f d\lambda = 0$ . The concept of hardening plasticity is employed for this work. The yield function  $f$  is then expressed as

$$f(\sigma_{ij}, h, T) = \sigma_v(\sigma_{ij}) - \sigma_{ys}^0(T) - h(\varepsilon_{eq}^p), \quad (4)$$

where  $\sigma_{ys}^0(T)$  is the initial yield stress as a function of temperature,  $h(\varepsilon_{eq}^p)$  the hardening function dependent on the equivalent plastic strain  $\varepsilon_{eq}^p$ , and  $\sigma_v$  is the von Mises stress given for general plane stress as

$$\sigma_v = \sqrt{\sigma_{xx}^2 - \sigma_{xx}\sigma_{yy} + \sigma_{yy}^2 + \sigma_{zz}^2 + 3\sigma_{xy}^2}. \quad (5)$$

### D. Lifetime predictions of the solder joint

The plastic strain caused by the temperature and different CTE of the materials used in the WLP, will eventually result in failure of the solder joint. To predict the number of temperature cycles a solder joint made with SAC305 can survive before it fails, the Coffin-Manson strain model for fatigue[12] is used. The number of life cycles to failure is calculated as

$$N_f = C(\Delta\varepsilon_{eq}^p)^{-\eta}, \quad (6)$$

where  $N_f$  is the number of cycles to failure,  $\Delta\varepsilon_{eq}^p$  is the difference in equivalent plastic strain, and  $C$  and  $\eta$  are 0.235 and 1.75 respectively[13].

### E. Finite Element Modeling

To simulate the thermal expansion and the subsequent stresses and strains in the solder joint, the Finite Element Method (FEM) is used. To ensure a proper result from the FEM simulations, the mesh and the boundary conditions must be properly defined.

The size of the mesh elements has a significant effect on the results of the simulations. Tsou et al.[13] found that the critical mesh size suitable for use in the Coffin-Manson strain method is to have an element with a length of  $12.5\mu\text{m}$  and a height of  $6.4\mu\text{m}$ , where the critical mesh is located in the top right of the solder ball. In accordance with these findings, the critical mesh size for the simulations performed here were set to the above mentioned dimensions for the two solder balls on the right. As the failures tend to occur furthest from the neutral point, i.e. on the right side of our model, the solder balls closer to the neutral point have been given a coarser mesh to reduce the computational cost.

To obtain proper boundary conditions the symmetry on the left side ( $x = 0$ ) of the model is taken into account. The movement in  $x$ -direction is fixed on the entire symmetry axis. Additionally, the  $y$ -direction for the bottom left side of the PCB is set to zero.

To collect the equivalent plastic strain required for machine learning part of this work, the equivalent plastic strain is determined for each time step at a predefined point. This predefined point is located in the top right of the solder ball, as that is generally where the highest plastic strain occurs in the WLP. This is in the same location as the critical mesh, emphasizing the importance of choosing the critical mesh. The FEM simulations were performed using the COMSOL Multiphysics® program. Unfortunately, due to time constraints the FEM model described in this section was not validated by any experiments. Nevertheless, the goal of this work is to prove results from FEM can be used for training an LSTM network.

The variables exported from the FEM simulations for use in the training of the PINNs are the equivalent plastic strain  $\varepsilon_{eq}^p$  as the value to predict, the stress components

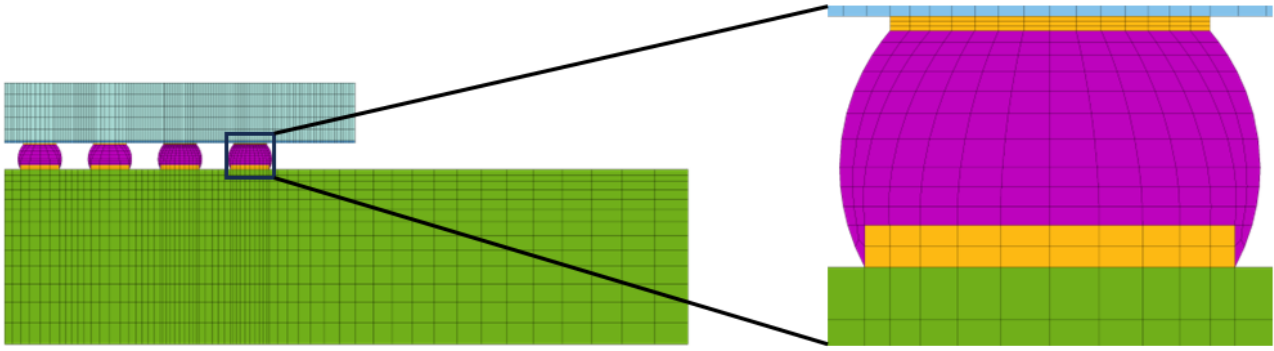


Fig. 4: The mesh used for the FEM simulation.

$\sigma_{xx}$ ,  $\sigma_{yy}$ ,  $\sigma_{zz}$  and  $\sigma_{xy}$  to be able to calculate the von Mises stress  $\sigma_v$  in Equation 5 and the yield function  $f$  from Equation 4 to use the condition that  $f \leq 0$  when training the model. Additionally, the current yield stress, i.e.  $\sigma_{ys}^0 + h(\varepsilon_{eq}^p)$ , and the von Mises stress  $\sigma_v$  are also collected from the simulations. How the data obtained from FEM is used in training the PINN is explained in the next section.

#### F. Model Training

This work leverages a Physics-informed Long Short-Term Memory (LSTM) network to predict the performance of solder joints in electronic components. The model is trained on data generated by high-fidelity FEM simulations as described in Section 2-E. To ensure compatibility with experimental settings and minimize required information, the model's inputs are restricted to ambient temperature along with its sinusoidal and cosinusoidal transformations. This choice enables the model to capture the influence of temperature variations on solder joint behavior while remaining computationally efficient.

A total of 66 simulations were conducted in COMSOL, each exploring different ramp rates and consequently resulting in varying strain and stress responses. For training purposes, 73,000 time steps were extracted from each simulation, ensuring that each captured at least three complete temperature cycles. To improve computational efficiency, the data underwent dimensionality reduction. Recognizing the repetitive nature of temperature, strain, and stress cycles, every 100th time step was selected, resulting in a significant reduction in data points.

The preprocessed data with the aforementioned transformations is fed into the model with an input shape of (730, 3). The model employs a single LSTM layer to process the sequential data. This layer transforms the input data into a higher dimensional representation with a size of 150. A tanh activation function is applied to the LSTM output, followed by a linear layer to generate the final output with a shape of (730, 5). The output values correspond to various stress components and the current yield stress Equation 4. Leveraging PyTorch's capabilities,

the model automatically calculates the gradients required within the flow rule equations. This enables the computation of crucial parameters like plastic strain and equivalent plastic strain. The value of 'lambda' is incorporated into the model as a trainable parameter, allowing it to be optimized alongside other model parameters.

### 3. Results and Discussion

The equivalent plastic strain as determined by the FEM simulations is shown for the solder joint in Figure 5. As expected the highest  $\varepsilon_{eq}^p$  occurs in the top right corner of the solder joint, in accordance with other FEM and experimental results[6, 13].

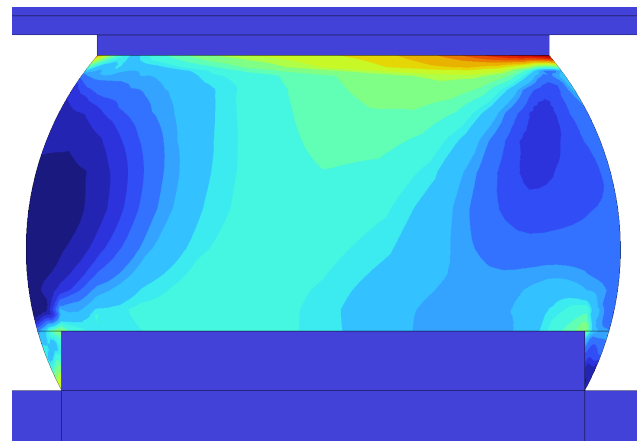


Fig. 5: Equivalent plastic strain  $\varepsilon_{eq}^p$  in the solder joint

The value of  $\varepsilon_{eq}^p$  is taken from a point in the top right of the solder joint for each timestep in the simulation. The result of which is used to train the model, as described in Section 2-F. An example of the equivalent plastic strain from the FEM simulation and its associated prediction, is shown in Figure 6. The predicted value follows the FEM results closely. The temperature cycles can even be observed for the early cycles. After which the model is able to follow the general upward trend of the plastic strain, leading to a very accurate predictions of the final  $\varepsilon_{eq}^p$  value. Furthermore, the individual stress components

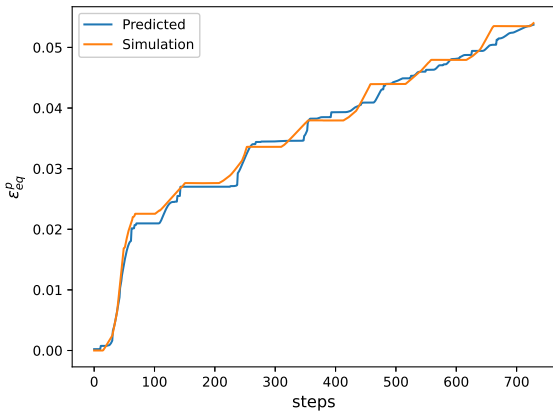


Fig. 6: The equivalent plastic strain  $\varepsilon_{eq}^p$  over time in a point.

$\sigma_{xx}$ ,  $\sigma_{yy}$ ,  $\sigma_{zz}$  and  $\sigma_{xy}$  have been plotted in Figures 7, 8, 9 and 10 respectively. The predicted stress components show good agreement with the FEM results. Thereby showcasing the capability of the proposed model to not only to predict the plastic strain, but also to generate accurate stress predictions for the solder joint.

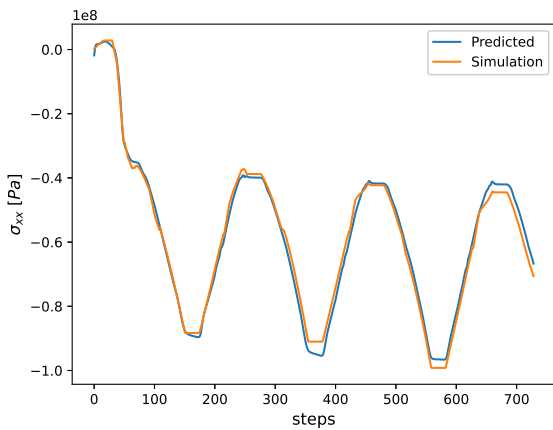


Fig. 7: The stress in  $x$ -direction  $\sigma_{xx}$ .

Additionally, the plastic strain multiplier  $d\lambda$  is predicted by the network, the result of which is shown in Figure 11. The value of  $d\lambda$  is mostly zero, which is to be expected as plasticity does not always occur. Another thing to notice is that the value is sometimes negative, violating the condition  $d\lambda \geq 0$ . However, it can be seen in Figure 6 that this does not lead to a negative trend in the plastic strain. The MSE loss function is shown in Figure 12. The drop at a 1000 epoch is due to a smaller learning rate at from that epoch onwards. Figure 13 shows difference in the predicted and simulated values for the equivalent plastic strain. The error does not have a general upward trend, indicating the stability of the proposed model over

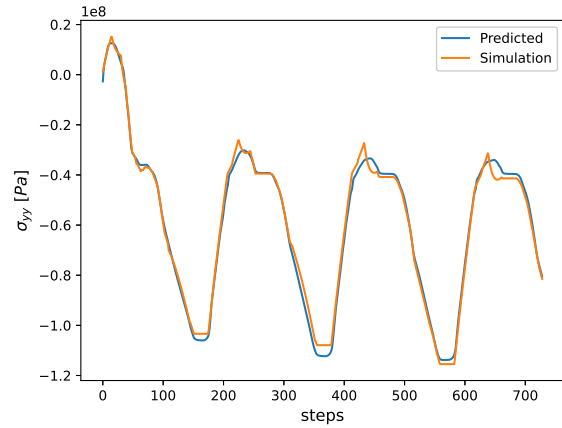


Fig. 8: The stress in  $y$ -direction  $\sigma_{yy}$ .

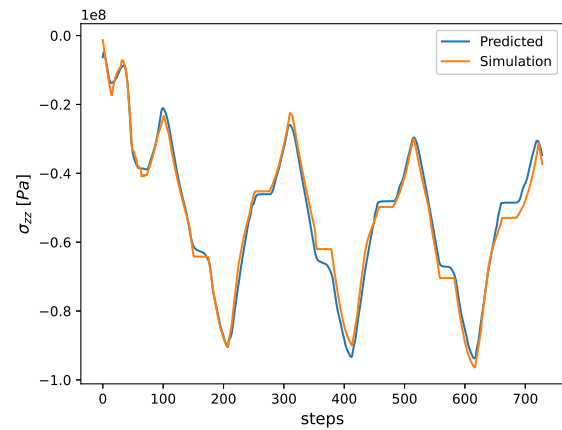


Fig. 9: The stress in  $z$ -direction  $\sigma_{zz}$ .

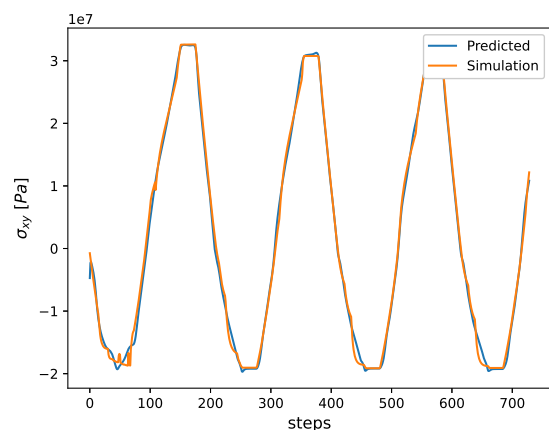


Fig. 10: The stress in  $xy$ -direction  $\sigma_{xy}$ .

time. The size of the error itself does not lead to significant inaccuracies when used for reliability predictions. Using the Coffin-Manson Equation 6 results in 699 and 716 cycles to failure for the simulated and predicted values respectively. This means the proposed method can also be used for lifetime predictions of the solder joint.

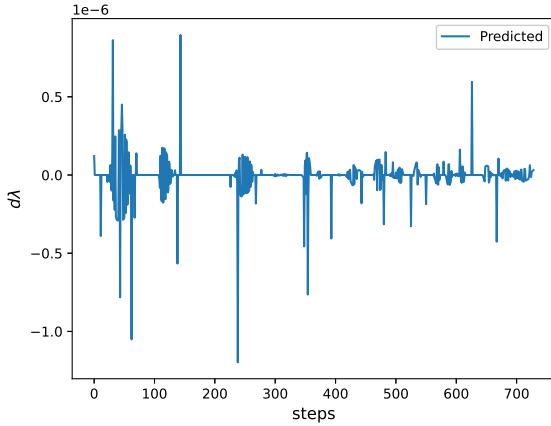


Fig. 11: Predicted value of  $d\lambda$ .

#### A. Discussion

This work demonstrated the use of physics-constrained neural network for qualifying solder joint reliability in WLP. The model was trained using data collected from a FEM simulation of the solder joint, to obtain the equivalent plastic strain in a point of interest. It was shown that the proposed model is capable of making accurate predictions. Nevertheless, some problems were encountered during the making of this work.

Firstly, as was already mentioned in Section 2-E, the finite element model was not validated by experimental results. This was not done due to time constraints. It is important to state that using the method proposed in

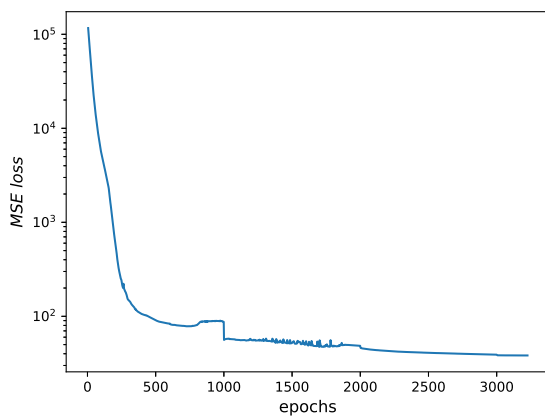


Fig. 12: Predicted value of MSE loss.

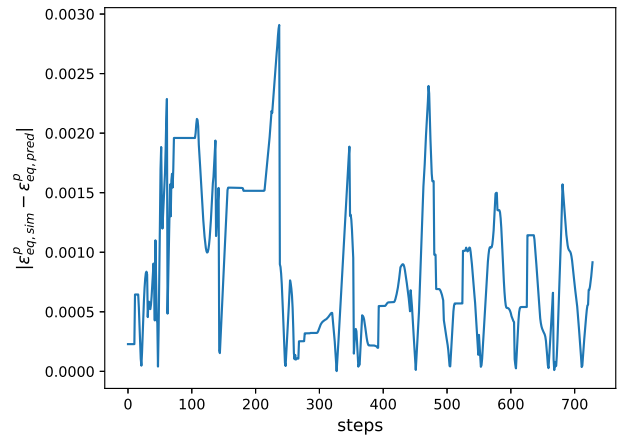


Fig. 13: The absolute value of the difference between the simulated and the predicted value of  $\varepsilon_{eq}^p$ .

this work will require experimentally validated training data to create accurate predictions usable for real world applications.

Another issue was encountered when trying to acquire the necessary data for use in the PINN equations. For example, when trying to calculate the equivalent plastic strain from the individual plastic strain components, it was found they are equal only when the specified point is on an integration point. A possible explanation for this is that Comsol applies the interpolation differently for different variables. Further understanding of the program, or possibly using a different program could remove this problem in the future. This would allow for using more advanced equations in PINNs, which would lead to a more efficient network and improved predictions.

Lastly, the plastic strain is predicted in a single point. It is well established the greatest plasticity occurs furthest away from the center, i.e. in the top right in this case. However, as the plastic strain is predicted only in a single point, this could cause slight under prediction of the plasticity. The maximum plasticity might not occur at the exact position of the point. Nevertheless, the difference between the predicted value and the actual maximum will not be significant if proper care is placed in deciding the location of the prediction point.

#### 4. Conclusion

The goal of this work was to exhibit the benefits of using machine learning for predicting the lifetime of a solder joint in a WLP. The conventional use of FEM simulations for these predictions are highly demanding in equipment as well as in expertise. To reduce the computational power and time required to obtain the equivalent plastic strain in the solder joint, a predictive model was trained using data obtained from FEM. The model employed a physics informed LSTM to increase accuracy and decrease training time. The proposed model

showed good agreement with the FEM results and was able to accurately predict the equivalent plastic strain as well as the stress components in the solder joint.

## 5. Acknowledgements

This research was carried out under project number N21006 in the framework of the Partnership Program of the Material innovation institute M2i ([www.m2i.nl](http://www.m2i.nl)) and the Dutch Research Council ([www.nwo.nl](http://www.nwo.nl)). This work is also supported by the project EXPLAIN, the Netherlands Enterprise Agency RVO under grant AI212001.

## References

- [1] Ming Chih Yew, Chan Yen Chou, and Kuo Ning Chiang. “Reliability assessment for solders with a stress buffer layer using ball shear strength test and board-level finite element analysis”. In: *Microelectronics Reliability* 47.9-11 SPEC. ISS. (Aug. 2007), pp. 1658–1662. ISSN: 00262714. DOI: 10.1016/j.microrel.2007.07.043.
- [2] Z.J. Xu et al. “Modeling of Board Level Solder Joint Reliability under Mechanical Drop Test with the Consideration of Plastic Strain Hardening of Lead-free Solder”. In: *2010 IEEE CPMT Symposium Japan*. 2010. ISBN: 9781424475940.
- [3] P. H. Hochstenbach et al. “Designing for reliability using a new Wafer Level Package structure”. In: *Microelectronics Reliability* 50.4 (Apr. 2010), pp. 528–535. ISSN: 00262714. DOI: 10.1016/j.microrel.2009.09.011.
- [4] Sunil Kumar Panigrahy et al. *An overview of ai-assisted design-on-simulation technology for reliability life prediction of advanced packaging*. Sept. 2021. DOI: 10.3390/ma14185342.
- [5] H.C. Kuo, B.R. Lai, and K.N. Chiang. “Study on Reliability Assessment of Wafer Level Package Using Design-on-Simulation with Support Vector Regression Techniques Nangang Exhibition Center”. In: *15th International Microsystems, Packaging, Assembly and Circuits Technology Conference (IMPACT)*. 2020. ISBN: 9781728198514.
- [6] H. Y. Hsiao and K. N. Chiang. “AI-assisted reliability life prediction model for wafer-level packaging using the random forest method”. In: *Journal of Mechanics* 37 (2020), pp. 28–36. ISSN: 18118216. DOI: 10.1093/jom/ufaa007.
- [7] P. H. Chou, K. N. Chiang, and Steven Y. Liang. “Reliability Assessment of Wafer Level Package using Artificial Neural Network Regression Model”. In: *Journal of Mechanics* 35.6 (Dec. 2019), pp. 829–837. ISSN: 18118216. DOI: 10.1017/jmech.2019.20.
- [8] Vahid Samavatian et al. “Correlation-driven machine learning for accelerated reliability assessment of solder joints in electronics”. In: *Scientific Reports* 10.1 (Dec. 2020). ISSN: 20452322. DOI: 10.1038/s41598-020-71926-7.
- [9] Yubiao Sun, Ushnish Sengupta, and Matthew Juniper. “Physics-informed deep learning for simultaneous surrogate modeling and PDE-constrained optimization of an airfoil geometry”. In: *Computer Methods in Applied Mechanics and Engineering* 411 (2023). ISSN: 00457825. DOI: 10.1016/j.cma.2023.116042.
- [10] M. Raissi, P. Perdikaris, and G. E. Karniadakis. “Physics-informed neural networks: A deep learning framework for solving forward and inverse problems involving nonlinear partial differential equations”. In: *Journal of Computational Physics* 378 (2019). ISSN: 10902716. DOI: 10.1016/j.jcp.2018.10.045.
- [11] Arunabha M. Roy and Suman Guha. “A data-driven physics-constrained deep learning computational framework for solving von Mises plasticity”. In: *Engineering Applications of Artificial Intelligence* 122 (2023). ISSN: 09521976. DOI: 10.1016/j.engappai.2023.106049.
- [12] L F Coffin and N Y Schenectady. *A Study of the Effects of Cyclic Thermal Stresses on a Ductile Metal*. Tech. rep. 1954. URL: [http://asmedigitalcollection.asme.org/fluidsengineering/article-pdf/76/6/931/6893676/931\\_1.pdf](http://asmedigitalcollection.asme.org/fluidsengineering/article-pdf/76/6/931/6893676/931_1.pdf).
- [13] C. Y. Tsou et al. “Reliability assessment using modified energy based model for WLCSP solder joints”. In: *2017 International Conference on Electronics Packaging, ICEP 2017*. Institute of Electrical and Electronics Engineers Inc., June 2017, pp. 7–12. ISBN: 9784990218836. DOI: 10.23919/ICEP.2017.7939312.